J|A|C|S
ARTICLES
Published on Web 01/21/2006

Detection of Second Hydration Shells in Ionic Solutions by XANES: Computed Spectra for Ni^{2+} in Water Based on Molecular Dynamics

Paola D'Angelo,*,† Otello Maria Roscioni,† Giovanni Chillemi,‡ Stefano Della Longa,§,|| and Maurizio Benfatto§

Contribution from the Dipartimento di Chimica, Università di Roma "La Sapienza", P. le A. Moro 5, 00185 Roma, Italy, CASPUR, Inter-University Consortium for Supercomputing in Research, via dei Tizii 6b, 00185 Roma, Italy, Laboratori Nazionali di Frascati, INFN, CP13, 00044 Frascati, Italy, and Dipartimento di Medicina Sperimentale, Universita dell'Aquila, Via Vetoio 67100 L'Aquila, Italy

Received September 11, 2005; E-mail: p.dangelo@caspur.it

Abstract: A general procedure to compute X-ray absorption near-edge structure (XANES) spectra within multiple-scattering theory starting from molecular dynamics (MD) structural data has been developed and applied to the study of a Ni^{2+} aqueous solution. This method allows one to perform a quantitative analysis of the XANES spectra of disordered systems using a proper description of the thermal and structural fluctuations. The XANES spectrum of Ni^{2+} in aqueous solution has been calculated using the structural information obtained from the MD simulations without carrying out any minimization in the structural parameter space. A very good reproduction of the experimental data was obtained including the second-shell water molecules in the calculation, thus showing that the second hydration shell provides a detectable contribution to the XANES spectra of ionic solutions. The analysis including the first-shell cluster only permitted us to quantitatively determine the effect of disorder on the amplitude of the XANES spectra for molecular complexes. These results simultaneously confirm the reliability of the procedure and the structural results obtained from MD simulations. The combination of MD and XANES is found to be very helpful to get important new insights into the quantitative estimation of structural properties of disordered systems.

1. Introduction

X-ray absorption spectroscopy (XAS) is a powerful experimental technique for local structural determination, which has been successfully applied to a large variety of systems. XAS spectra have been typically split into a low-energy region, termed XANES (X-ray absorption near-edge structure), and a region which extends from about 50 eV to more than 1000 eV above the edge, which is called EXAFS (extended X-ray absorption fine structure).[1]

During the last 20 years, much effort has been made to develop a reliable theoretical scheme to extract metrical and angular information from the EXAFS spectra.[2,3] One of the major applications of this spectroscopy is the determination of the structure of disordered systems even if, in the case of condensed matter lacking long-range order, the fitting parameters are often correlated and the EXAFS data analysis can lead to ambiguous results.[4] A strategy to help in the extraction of structural details contained in the EXAFS spectra of disordered systems is to include independent information derived from computer simulations. A theoretical approach, which uses pair distribution functions obtained from molecular dynamics (MD) simulations to model the EXAFS signal, has been recently developed and successfully applied to the quantitative structural investigation of ionic solutions.[5,6] These studies, mainly dealing with divalent transition metal ions, have shown that the EXAFS spectroscopy is an elective technique for elucidating the structure of the first coordination shell of ionic solutions.

Conversely, a combined experimental and theoretical study of Zn^{2+}, Ni^{2+}, and Co^{2+} aqueous solutions has shown that second-shell contributions are not detectable by EXAFS,[6,7] although some authors have claimed that the second hydration shell of some cations such as Cr^{3+}, Zn^{2+}, and Rh^{3+} is observable by this technique.[8−10]

† Università di Roma "La Sapienza".
‡ CASPUR.
§ Laboratori Nazionali di Frascati.
|| Universita dell'Aquila.

(1) Sayers, D. E.; Stern, A.; Lytle, F. W. *Phys. Rev. Lett.* **1971**, *27*, 1204.
(2) Rehr, J. J.; Albers, R. C. *Rev. Mod. Phys.* **2000**, *72*, 621.
(3) Filipponi, A. *J. Phys. Condens. Matter* **2001**, *13*, R23.
(4) D'Angelo, P.; Di Nola, A.; Mangoni, M.; Pavel, N. V. *J. Chem. Phys.* **1996**, *104*, 1779.
(5) D'Angelo, P.; Di Nola, A.; Filipponi, A.; Pavel, N. V.; Roccatano, D. *J. Chem. Phys.* **1994**, *100*, 985.
(6) D'Angelo, P.; Barone, V.; Chillemi, G.; Sanna, N.; Meyer-Klaucke, W.; Pavel, N. V. *J. Am. Chem. Soc.* **2002**, *124*, 1958.
(7) Chillemi, G.; D'Angelo, P.; Pavel, N. V.; Sanna, N.; Barone, V. *J. Am. Chem. Soc.* **2002**, *124*, 1958.
(8) Muñoz-Páez, A.; Pappalardo, R. R.; Sánchez Marcos, E. *J. Am. Chem. Soc.* **1995**, *117*, 11710.
(9) Lindqvist-Reis, P.; Muñoz-Páez, A.; Díaz-Moreno, S.; Pattanaik, S.; Person, I.; Sandström, M. *Inorg. Chem.* **1998**, *37*, 6675.
(10) Sakane, H.; Muñoz-Páez, A.; Díaz-Moreno, S.; Martinez, J. M.; Pappalardo, R. R.; Sánchez Marcos, E. *J. Am. Chem. Soc.* **1998**, *120*, 10397.

10.1021/ja0562503 CCC: $33.50

The XANES spectra are sensitive both to geometrical and electronic properties of the photoabsorber atom, and the low-energy region is dominated by multiple scattering (MS) effects, owing to the low kinetic energy of the photoelectron. In contrast with EXAFS, the XANES spectroscopy has been hardly used to investigate ionic solutions, whereas several studies on pure water have recently appeared in the literature.[11]

Recently, a new method (MXAN) of extracting the metrical and angular structural information available in XANES spectra has been developed[12] in the framework of the MS theory and successfully applied to the analysis of several systems, both in the solid and liquid state, allowing a quantitative extraction of the relevant geometrical information about the absorbing site.[12−15] However, in the case of ionic solutions, the XANES spectra have been calculated considering only the environment formed by the first coordination shell. This approach is usually adopted because the contribution from molecules and arrangements instantaneously distorted cannot be calculated using the standard XANES data analysis methods. A possible strategy to overcome this problem is to analyze the XANES spectra using a microscopic description of the system derived from MD simulations. As previously mentioned, this approach has been extensively used for the analysis of the EXAFS energy region, although only qualitative applications have been performed, up to now, for the XANES spectra in the framework of the MS theory.[16] Recently, XANES spectra of pure water have been calculated in the framework of full-potential techniques, using first-principle MD to account for the effects of dynamics.[17]

The aim of this paper is to perform a quantitative treatment of disorder effects on XANES and to establish whether the second hydration shell provides a detectable contribution to the XANES spectra of ionic solutions. To this end, an iterative procedure which uses MXAN and MD simulations to generate a configurational averaged XANES spectrum has been developed and applied to the investigation of the Ni^{2+} ion in aqueous solution.

Our methodology demonstrates, on one hand, that the second hydration shell provides a detectable contribution to the XANES spectra of ionic solution and, on the other hand, that it is possible to perform a quantitative analysis of the XANES region of disordered systems, thus making possible the acquisition of structural and geometrical information not accessible by other experimental techniques.

2. Methods

2.1. Experimental Data. A 0.2 M Ni^{2+} aqueous solution was obtained by dissolving the appropriate amount of $Ni(NO_3)_2$ in water. XAS spectra at the Ni K-edge were recorded in transmission mode using the EMBL spectrometer at DESY.[18] The spectra were collected at room temperature with a Si(111) double-crystal monochromator, and 50% harmonic rejection was achieved by slightly detuning the two crystals from parallel alignment. Three spectra were recorded and averaged after performing an absolute energy calibration.[19,20] The DORIS III storage ring was running at an energy of 4.4 GeV with positron currents between 70 and 40 mA. The solution was kept in a cell with Kapton film windows and Teflon spacers of 1 mm.

2.2. Molecular Dynamics Details. The XANES spectrum of Ni^{2+} aqueous solution has been analyzed starting from the microscopic description of the system derived from a MD simulation that was already successfully used to interpret the EXAFS region of the spectrum.[6,7] This MD simulation was carried out using a novel procedure starting from the generation of an effective two-body potential from quantum mechanical ab initio calculations in which the many-body ion−water terms are accounted for by the polarizable continuum model.[21] This approach is computationally very efficient and allows one to carry out long MD simulations, indispensable to reproduce the dynamic properties of the second hydration shell of the Ni^{2+} ion. A thorough description of both the procedure and the MD simulation results can be found in refs 7 and 22. Our effective two-body potential provides structural results that are in excellent agreement with the most recent experimental determinations carried out with neutron diffraction,[23] X-ray diffraction,[24] and X-ray absorption measurements.[25] A recent combined quantum mechanical−molecular mechanical MD simulation delivers the same coordination numbers for both first and second hydration shells, as compared to the experimental studies, but a slightly longer Ni−O distance.[26]

The simulation has been carried out using a modified version of the GROMACS package version 1.51.[27] The system consists of one Ni^{2+} ion and 819 SPC/E water molecules. A cutoff of 12 Å was used for the pair interactions, updating the neighboring pair list every 10 steps. To simulate a canonical ensemble, the temperature was kept fixed at 300 K by weak coupling to an external temperature bath with a coupling constant of 0.1 ps.[28] The system was equilibrated for 50 ps and simulated for 1 ns with a time step of 2 fs. The trajectory was saved every 25 time steps for analysis, which was carried out using in-house written codes.

Figure 1 shows the Ni^{2+}−water radial distribution functions ($g(r)$) and the corresponding running integration numbers obtained from MD calculations.

The ion−O and ion−H $g(r)$'s show very sharp and well-separated first peaks, indicating the presence of a well-organized nearest-neighbor hydration shell. Note that the ion−H $g(r)$ first peak falls in a region

(11) Smith, J. D.; Cappa, C. D.; Wilson, K. R.; Messer, B. M.; Cohen, R. C.; Saykally R. J. *Science* **2004**, *306*, 851; Wernet, Ph.; Nordlund, D.; Bergmann, U.; Cavalleri, M.; Odelius, M.; Ogasawara, H.; Näslund, L.-Å.; Hirsch, T. K.; Ojamäe, L.; Glatzel, P.; Pettersson, L. G. M.; Nilsson, A. *Science* **2004**, *304*, 995; Nilsson, A.; Wernet, Ph.; Nordlund, D.; Bergmann, U.; Cavalleri, M.; Odelius, M.; Ogasawara, H.; Näslund, L.-Å.; Hirsch, T. K.; Ojamäe, L.; Glatzel, P.; Pettersson, L. G. M. *Science* **2005**, *308*, 793a; Wilson, K. R.; Cavalleri, M.; Rude, B. S.; Schaller, R. D.; Catalano, T.; Nilsson, A.; Saykally, R. J.; Pettersson, L. G. M. *J. Phys. Chem. B* **2005**, *109*, 10194; Messer, B. M.; Cappa, C. D.; Smith, J. D.; Wilson, K. R.; Gilles, M. K.; Cohen, R. C.; Saykally, R. J. *J. Phys. Chem. B* **2005**, *109*, 5375; Cappa, C. D.; Smith, J. D.; Wilson, K. R.; Messer, B. M.; Gilles, M. K.; Cohen, R. C.; Saykally, R. J. *J. Phys. Chem. B* **2005**, *109*, 7046; Näslund, L.-Å.; Luning, J.; Ufuktepe, Y.; Ogasawara, H.; Wernet, P.; Bergmann, U.; Pettersson, L. G. M.; Nilsson, A. *J. Phys. Chem. B* **2005**, *109*, 13835; Näslund, L.-Å.; Edwards, D. C.; Wernet, P.; Bergmann, U.; Ogasawara, H.; Pettersson, L. G. M.; Myneni, S.; Nilsson, A. *J. Phys. Chem. A* **2005**, *109*, 5995.

(12) Benfatto, M.; Della Longa, S. *J. Synchrotron Radiat.* **2001**, *8*, 1087.

(13) Benfatto, M.; Della Longa, S.; Natoli, C. R. *J. Synchrotron Radiat.* **2003**, *10*, 51.

(14) D'Angelo, P.; Benfatto, M.; Della Longa, S.; Pavel, N. V. *Phys. Rev. B: Condens. Matter Mater. Phys.* **2002**, *66*, 064209.

(15) Della Longa, S.; Arcovito, A.; Girasole, M.; Hazemann, J. L.; Benfatto, M. *Phys. Rev. Lett.* **2001**, *87*, 155501.

(16) Merkling, P. J.; Muñoz-Páez, A.; Marcos, E. S. *J. Am. Chem. Soc.* **2002**, *124*, 10911.

(17) Hetényi, B.; De Angelis, F.; Giannozzi, P.; Car, R. *J. Chem. Phys.* **2004**, *120*, 8632; Cavalleri, M.; Odelius, M.; Nordlund, D.; Nilsson, A.; Pettersson, L. G. M. *Phys. Chem. Chem. Phys.* **2005**, *7*, 2854.

(18) Hermes, C.; Gilberg, E.; Koch, M. H. *Nucl. Instrum. Methods Phys. Res.* **1984**, *222*, 207.

(19) Pettifer, R. F.; Hermes, C. *J. Appl. Crystallogr.* **1985**, *18*, 404−412.

(20) Pettifer, R. F.; Hermes, C. *J. Phys. Colloq.* **1986**, *47*, C8−127.

(21) Amovilli, C.; Barone, V.; Cammi, R.; Cances, E.; Cossi, M.; Mennucci, B.; Pomelli, C. S., Tomasi, J. *Adv. Quantum Chem.* **1999**, *32*, 227.

(22) Chillemi, G.; Barone, V.; D'Angelo, P.; Mancini, G.; Persson, I.; Sanna, N. *J. Phys. Chem. B* **2005**, *109*, 9186.

(23) Neilson, G. W.; Ansell, S.; Wilson, J. *Z. Naturforsch., A: Phys. Sci.* **1994**, *50*, 247.

(24) Ohtaki, H.; Radnai, T. *Chem. Rev.* **1993**, *93*, 1157.

(25) Wallen, S. L.; Palmer, B. J.; Fulton, J. L. *J. Chem. Phys.* **1998**, *108*, 4039.

(26) Inada, Y.; Mohammed, A. M.; Loeffler, H. H.; Rode, B. M. *J. Phys. Chem. A* **2002**, *106*, 6783.

(27) Berendsen, H. J. C.; van der Spool, D.; van Drunen, R. *Comput. Phys. Commun.* **1995**, *91*, 43.

(28) Berendsen, H. J. C.; Postma, J. P. M.; Di Nola, A.; Haak, J. R. *J. Chem. Phys.* **1984**, *81*, 3684.

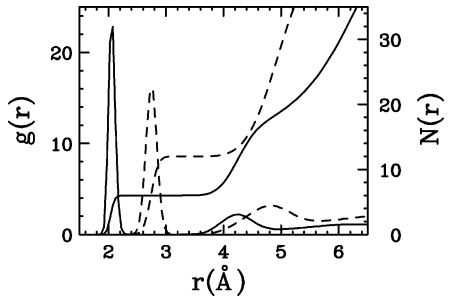

Figure 1. Ion−oxygen (full line) and ion−hydrogen (dashed line) pair distribution functions as derived from MD simulations for Ni^{2+} aqueous solutions (left scale) and corresponding running integration numbers (right scale).

where no ion−O contacts are present. This indicates the existence of a preferential orientation of the water molecules in the first solvation shell. The integration over the ion−O first peak gives a coordination number of six in agreement with the existence of an octahedral structure around the ion. The number of water molecules in the second hydration shell, which is not easily accessible from experiments, can be estimated from the simulation. Integration of the MD Ni^{2+}−O $g(r)$ second peak indicates that the second hydration shell contains about twice the number of molecules of the first shell.[6] During the 1 ns simulation, no water molecules in the first hydration shell exchanged with the second hydration shell. The residence time of water molecules in the second hydration shell is 10.3 ps, calculated following the method of Impey and coauthors[29] and considering a distance cutoff of 5 Å for the ion−oxygen distance.

2.3. XANES Data Analysis. The XANES calculations have been performed using a new software procedure named MXAN.[12,13,15] The X-ray photoabsorption cross section is calculated using the full MS scheme in the framework of the muffin-tin approximation for the shape of the potential. The exchange and correlation part of the potential is determined on the basis of the local density approximation of the self energy. The real part of self energy is calculated by using the Hedin−Lundqvist (HL) energy-dependent potential, whereas all inelastic processes are accounted for by convolution with a broadening Lorentzian function having an energy-dependent width of the form $\Gamma(E) = \Gamma_c + \Gamma_{mfp}(E)$. The constant part Γ_c accounts for both the core-hole lifetime and the experimental resolution, whereas the energy-dependent term represents all the intrinsic and extrinsic inelastic processes.[12,13,15]

In the first step of the analysis, the XANES spectrum has been computed considering only the first hydration shell around the Ni^{2+} ion. In this case, 6 oxygen and 12 hydrogen atoms have been included in the calculation. Additional analyses have been performed including the second hydration shell, and 19 oxygens and 36 hydrogens have been included as scatterer atoms using the geometry and the orientation of each MD snapshot. The importance of the hydrogen contribution in the calculation of the XANES spectrum of Ni^{2+} in aqueous solution has been outlined in ref 14. The potential has been calculated using muffin-tin radii of 0.2, 0.9, and 1.2 Å for hydrogen, oxygen, and nickel, respectively.

2.4. Computational Procedure. XANES spectra of the Ni^{2+} aqueous solution have been calculated starting from the microscopic structure derived from MD simulations. A direct method to obtain the proper configurational average of the X-ray absorption cross section is to calculate several theoretical XANES spectra from distinct MD snapshots and to generate an averaged spectrum accounting for thermal and structural disorder.

In the first step of the analysis, a trajectory containing only the nickel ion and its first hydration shell has been extracted from the total MD trajectory. Each snapshot has been used to generate the XANES associated with the corresponding instantaneous geometry, and the averaged theoretical spectrum has been obtained by summing all the spectra and dividing by the total number of MD snapshots used. At this stage, only the real part of the HL potential has been used; i.e., theoretical spectra do not account for any intrinsic and extrinsic inelastic process, whereas the damping associated with the core hole lifetime of the nickel atom has been accounted for in the calculation by convoluting the spectra with a constant Lorentzian function ($\Gamma_c = 1.44$ eV).

In the second step of the analysis, the influence of the second hydration shell on the XANES spectrum of Ni^{2+} has been assessed. To this end, a trajectory containing the ion and the first nineteen water molecules has been extracted from the total MD trajectory. In the MXAN calculation, we included all the water molecules separated from the cation by a distance shorter than 4.5 Å because water molecules at larger distances have been found to provide a negligible contribution. Also, in this case, several spectra have been calculated and averaged starting from the instantaneous configurations obtained from the MD calculations.

An important question when dealing with the computation of spectra from MD simulations is to determine the total sampling length that is necessary to have a statistically significant average. To this end, we performed an over-sampled average of both the first-shell, and first- and second-shell spectra using 10 000 configurations, and we calculated a residual function defined as the difference between the incremental averaged spectrum and the over-sampled spectrum. A residual value of 10^{-5} was chosen to establish the number of spectra which are necessary to have a statistically significant average. As a result, we found that 130 and 400 configurations are the lower limits when considering the first-, and first- and second-shells, respectively.

An IBM SP3 (16x PW3@375 MHz) parallel machine has been used, and the execution time for a single MXAN calculation was 60 s for a first-shell-only cluster and 20 min for a first-plus-second-shell cluster. We exploited the embarrassing parallel characteristic of the procedure to independently perform 16 MXAN calculations contemporaneously. The total calculation time for 10 000 first-shell XANES spectra was then reduced to about 10 h, whereas the total calculation time for 10 000 first- and second-shell XANES calculations was 350 h. On the other hand, the calculation time for 130 first-shell and 400 first- and second-shell spectra was about 2 and 14 h, respectively, and this can be taken as an indicative time for other transition metal water solutions.

3. Results

3.1. First-Shell Contribution. The inner hydration shell of Ni^{2+} is well-known to have an octahedral structure with six tightly bound water molecules. The structural disorder within the first hydration shell is derivable from fluctuations of the water molecules around the absorber atom, as determined from the MD simulations. This microscopic description of the solution enables an "a priori" estimation of the damping associated with the structural disorder, which is typically expressed through the Debye−Waller (DW) factor. The averaged theoretical spectrum associated with the octahedral hydration complexes obtained from the MD simulation is shown in Figure 2, together with two individual instantaneous structures. The calculated XANES spectra present noticeable differences all along the energy range, showing the sensitivity of the XANES spectra to geometrical changes. As expected, the main differences are present for energy values higher than 25 eV, where the structural contribution dominates, and this shows the importance of making a proper sampling of the configurational space. A deeper insight into the effect of thermal disorder on the XANES spectra of first-shell hydration complexes has been obtained by comparing the averaged total XANES spectrum with the spectrum calculated using a unique, rigid octahedral model with Ni−O

(29) Impey, R. W.; Madden, P. A.; McDonald, I. R. *J. Phys. Chem.* **1983**, *87*, 5071.

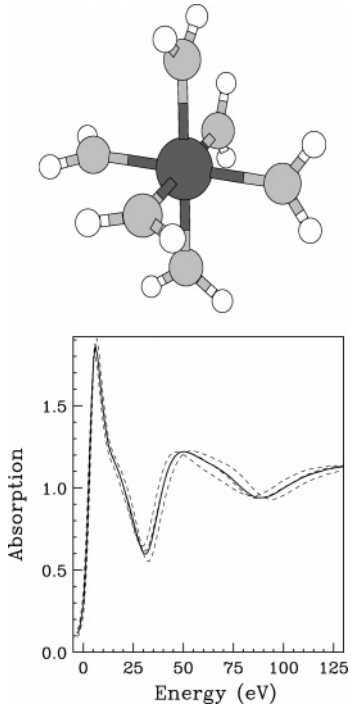

Figure 2. Comparison of the theoretical XANES spectrum obtained from the MD average including the first hydration shell (solid line) and two spectra associated with individual MD configurations (dashed line). Upper panel: symmetrical first-shell hydration complex of Ni^{2+}.

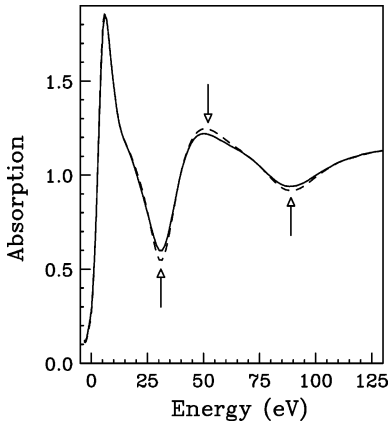

Figure 3. Comparison of the theoretical XANES spectrum obtained from the MD average including the first hydration shell (solid line) and a single theoretical XANES spectrum computed from a symmetrical first-shell cluster (dashed line).

distances of 2.03 Å (see Figure 3). The interesting fact derived from Figure 3 is that the structural disorder has a small effect on the XANES spectrum, and differences are only evident in the energy range above 25 eV, in agreement with the exponential trend of the thermal damping factor.

This result is not surprising as the Ni^{2+} ion forms a quite-stable hydration complex, and fluctuations of the first-shell water molecules are due only to the thermal motion. In the case of alkali metal ion aqueous solutions, where the mean-residence time of water molecules in the first hydration shell is very short, the hydration sphere is highly diffuse and poorly defined, and the corresponding damping effect is expected to be much stronger.

3.2. Second-Shell Contribution. Structural and dynamic information on the second hydration shell of ions is much poorer

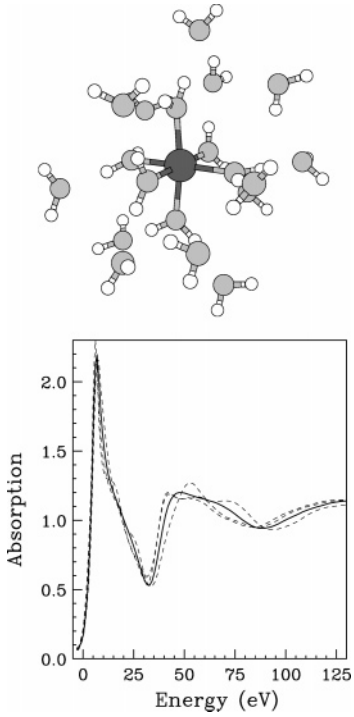

Figure 4. Comparison of the theoretical XANES spectrum obtained from the MD average including the first and second hydration shells (solid line) and three spectra associated with individual MD configurations (dashed line). Upper panel: typical first and second-shell hydration cluster.

than that of the first shell as the quantitative analysis of radial distribution curves in the long distance range is difficult and much less reliable. Until now, X-ray diffraction has been the principal source of structural information on the second shell,[24] although the contradictory results present in the literature indicate that it is not exempt from arbitrariness. More reliable information on the structure of the second shell may be obtained by isomorphous substitution methods in X-ray diffraction and isotopic substitution methods in neutron diffraction measurement.[31] Of course, such methods cannot be applied to every electrolyte solution. In this contest, the possibility of using the XANES technique to gain structural information on the second coordination shell of transition metal ions in water solutions is very interesting.

As outlined above, the second hydration shell contribution to the XANES spectrum can be calculated starting from the microscopic configurations derived from the MD calculations. In particular, our MD simulation suggests the presence of a second shell formed by about 13 water molecules at about 4.27 Å. The coordination number and the mean square deviation agree well with the average values provided by XRD and ND studies,[24] reinforcing the reliability of the MD structural results.

The XANES total theoretical spectrum obtained from 400 MD snapshots including both the first and second shell is shown in Figure 4, together with three spectra computed from instantaneous configurations. In this case, the individual spectra show marked differences both in the edge and in the higher-energy region. Several peculiar features are present in the individual spectra, which are due to the second-shell local geometries. All these structural peaks are smeared out in the

(30) Roscioni O. M.; D'Angelo, P.; Chillemi, G.; Della Longa, S.; Benfatto, M. *J. Synchrotron Radiat.* **2005**, *12*, 75.
(31) Enderby, J. E. *Chem. Soc. Rev.* **1995**, *24*, 159.

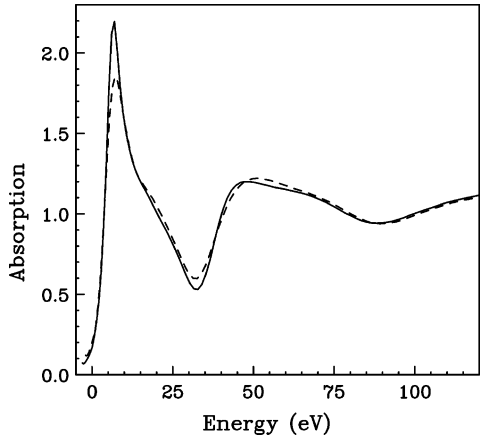

Figure 5. Comparison of the theoretical XANES spectrum obtained from the MD average including the first hydration shell (dashed line) and the averaged theoretical XANES spectrum including the first and second shells (solid line).

averaged spectrum, which shows the characteristic oscillations observed in the experimental data. Considering the large deviation among instantaneous spectra, it seems unlikely that a single representative configuration can be used to model the experimental data.

A deeper insight into the effect of the second hydration shell on the XANES spectrum of Ni^{2+} can be gained by the direct comparison between the averaged spectrum calculated using first-shell-only and the first- and second-shell clusters (see Figure 5). Significant differences appear in the low-energy region up to about 60 eV from the threshold. In particular, the edge intensity is lowered in the spectrum containing only the first-shell water molecules, which exhibits a different shape in the region around the first minimum. The two spectra become identical for energy values higher than 60 eV, and this finding underlines the insensitivity of the EXAFS technique toward second-shell contributions.

4. Discussion

The combined MD-XANES analysis performed in the present study clearly shows that the second-shell water molecules provide a detectable contribution to the XANES spectrum of Ni^{2+} in water. Nevertheless, to assess the reliability of the entire procedure, it is necessary to compare the total averaged XANES spectra with the experimental data. To this end, all inelastic processes have been accounted for by convoluting the theoretical averaged spectra with a broadening Lorentzian function, and the corresponding nonstructural parameters have been optimized. The agreement between the experimental and theoretical data has been assessed by the goodness-of-fit parameter (R_{sq}), as described in ref 12.

In the upper panel of Figure 6, the experimental XANES data are compared with the averaged theoretical spectrum including the first-shell water molecules only. The overall agreement of the two spectra is good even if the first rising peak of the theoretical spectrum is slightly over damped as compared with the experimental one. Moreover, the shape of the spectrum at about 18 eV is not completely reproduced. In this case, the R_{sq} value obtained from the minimization is 3.5. In the lower panel of Figure 6, the averaged theoretical spectrum including both the first and the second hydration shell is compared with the experimental spectrum. In this case, the agreement between

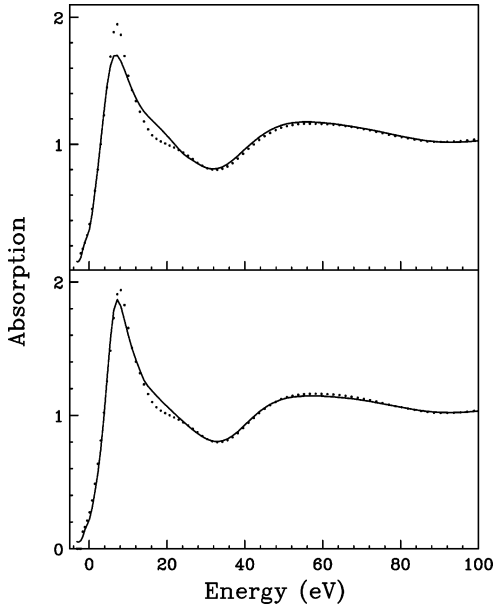

Figure 6. Upper panel: Comparison between the averaged theoretical XANES spectrum including the first shell (solid line) and the experimental data (dotted line) of Ni^{2+} in water solution. Lower panel: Comparison between the averaged theoretical XANES spectrum including the first and second shell (solid line) and the experimental data (dotted line) of Ni^{2+} in water solution.

calculated and experimental data is much better; the intensity of the peak after the main edge resonance is almost reproduced, and the hump at about 18 eV is smeared out. The R_{sq} value is 2.0, showing the improvement obtained with the inclusion of the higher distance contribution. It is important to outline that the XANES spectrum has been calculated using the structural information obtained from the MD simulations without carrying out any minimization in the structural parameter space. To the best of our knowledge, this is the first time that a XANES spectrum has been quantitatively reproduced in a wide energy range using the dynamical description of the system obtained from a simulation. Thus, when second-shell contributions are included in potential and full MS calculations, the shape of the averaged theoretical spectrum is much more similar to the experimental one.

The final appearance of the shoulder at 18 eV and of the height and shape of the rising peak is the result of the second-shell structural contribution obtained from the statistical average introduced by the set of MD snapshots used to compute the individual spectra. This finding supports strongly the need to include statistical structural information on the second coordination shell to correctly reproduce the experimental data. As previously observed, the XANES structures are extremely sensitive to the second-shell local geometries, and a thorough sampling of the configurational space has to be made to perform a correct analysis. Therefore, although a single representative configuration can be used to model the first hydration shell, this approach cannot be adopted to include the effect of higher shells.

A last remark we would like to make concerns the approximations used to calculate the XANES spectra. As previously mentioned, all of the calculations have been performed in the framework of the muffin-tin approximation, and this could be the origin of the discrepancies between the theoretical and experimental spectra as evident from the lower panel of Figure

6. To investigate the effect of the muffin-tin approximation, we performed a preliminary full-potential first-shell calculation using a fixed octahedral configuration and optimizing the nonstructural parameters only. As a result, the shape of the spectrum slightly changes, especially in the low-energy region, showing that the muffin-tin approximation has some effect. Nevertheless, up to now, an averaged spectrum including the second hydration shell cannot be calculated using a full-potential procedure within the MS theory due to the extremely long computational time require for a single calculation.

In conclusion, we have developed a general procedure to calculate a configurational averaged XANES spectrum directly from the geometrical configurations generated from MD simulations. Theoretical XANES spectra have been calculated with the MXAN code, and the procedure has been applied to a Ni^{2+} aqueous solution. A parallel execution of MXAN has been performed, allowing a substantial reduction of the calculation time.

This approach, applied to the first-shell cluster, allowed us to quantitatively determine the effect of disorder on the amplitude of the XANES spectra for molecular complexes. In this case, the DW effect has been found to provide a very small contribution, thus confirming the reliability of the MXAN procedure.

A very good reproduction of the experimental spectrum has been obtained including the second-shell water molecules in the calculation. The XANES spectrum of Ni^{2+} aqueous solution is strongly influenced by the second hydration shell, but in this case, the importance of fluctuations of the structure around the absorber atom forces one to take them into account when calculating the XANES.

In the case of disordered systems, whereas the EXAFS data can be interpreted using a model average structure and accounting for the disorder with the DW factor, the results presented here indicate that this approach is not completely reliable for the XANES region of the spectrum, because in this case, the second hydration shell provides a clearly detectable contribution. Therefore, the combination of MD simulations and XANES may provide new important structural insights into the high distance range of liquid samples and biological media.

Acknowledgment. We thank CASPUR for technical support.

JA0562503